Supplementary Figure 1. Effect of CNO on suppression of DGC activity

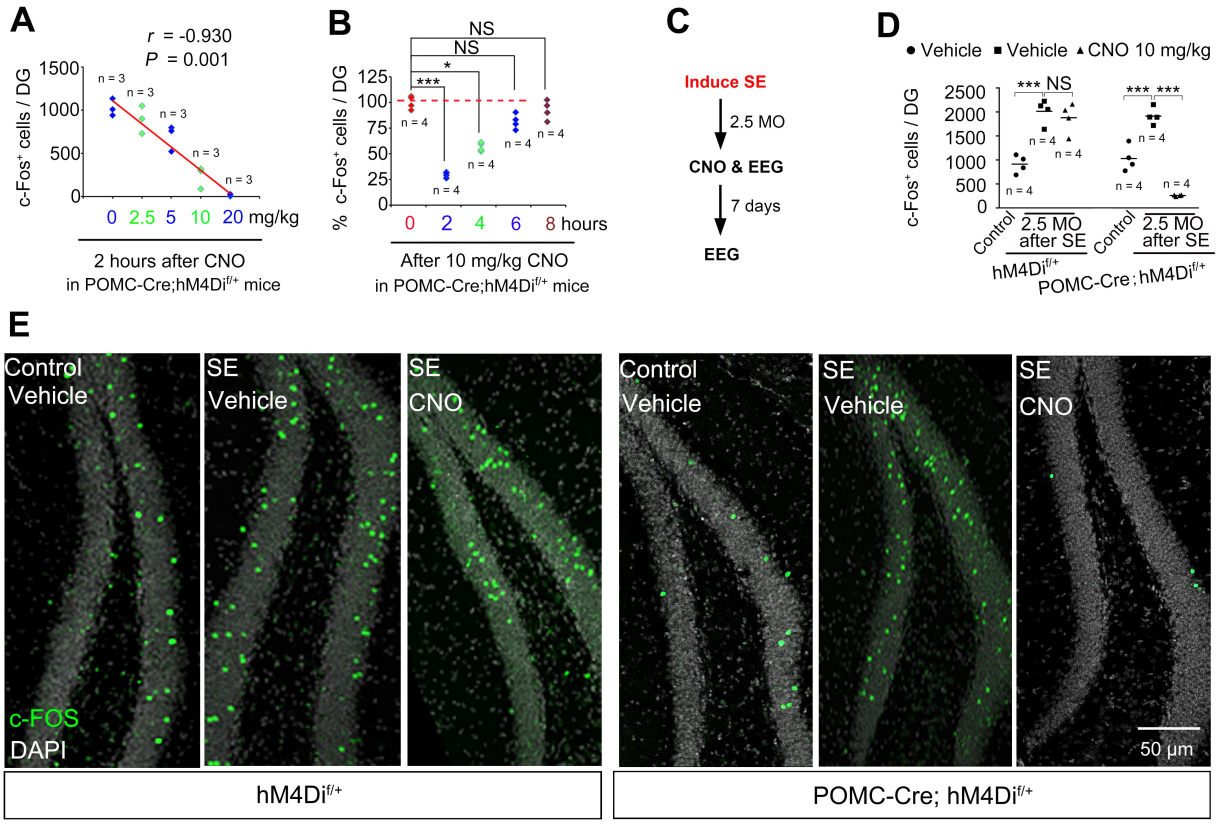

A. The number of c-FOS$^+$ cells shows the efficacy of suppression of DGC activity in a CNO dose-dependent manner (n =3, each). **B**. CNO (10 mg/kg) sufficiently reduces c-FOS$^+$ cells, and its effect is transient and reversible (n = 4, each). **C**. A schematic showing the timeline of SE induction, EEG monitoring, and CNO treatment. **D-E.** CNO treatment significantly reduced c-FOS$^+$ cells in epileptic POMC-Cre;hM4Di$^{f/+}$ mice, but not in hM4Di$^{f/+}$ control mice (n =4, each). Data represent mean ± SEM. *P < 0.05 and ***P < 0.001, as determined by a Pearson Correlation (A), Kruskal-Wallis tests with Dunn's multiple comparison tests (B), and two-way ANOVAs with Bonferroni's multiple comparison tests (D). NS = "non-significant"

Supplementary Figure 2. CNO specifically suppresses DGCs in POMC-Cre;hM4Di$^{f/+}$ mice

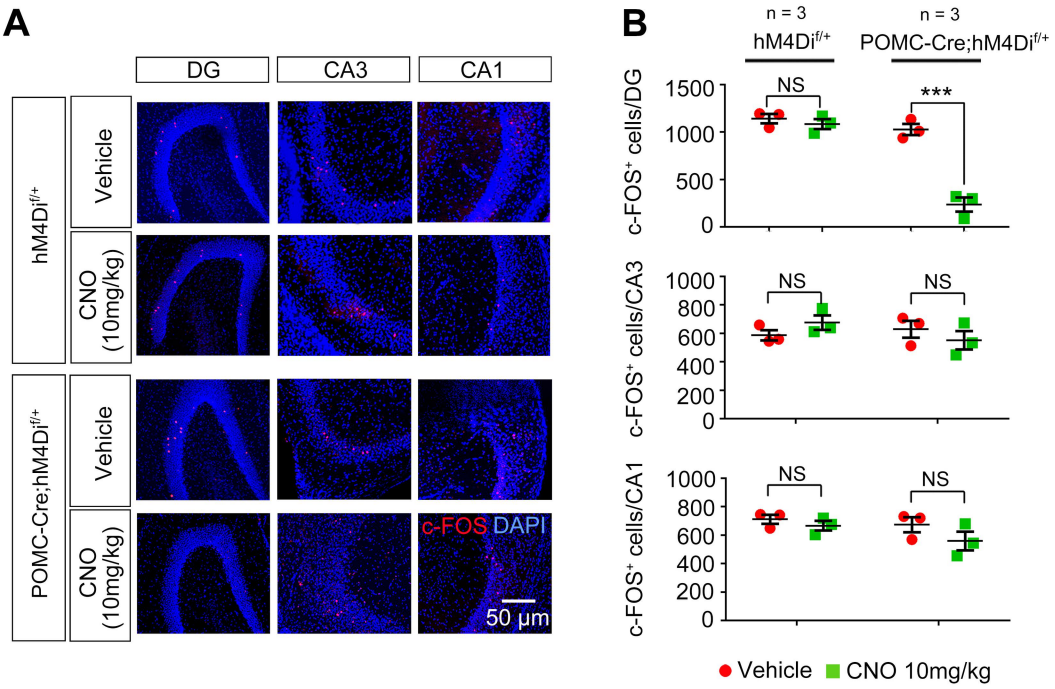

A. Representative photos show that CNO treatment reduces c-FOS expression in the dentate gyrus, but not in CA3 or CA1, of POMC-Cre;hM4Di$^{f/+}$ mice. **B.** The number of c-FOS$^+$ cells was significantly reduced in the dentate gyrus, but not in CA3 and CA1, of POMC-Cre;hM4Di$^{f/+}$ mice following 10 mg/kg CNO (green), while none of these measures were significantly altered in hM4Di$^{f/+}$ control mice (n = 3, each) . Data represent mean ± SEM. ***P < 0.001, as determined by two-way ANOVAs with Bonferroni's multiple comparisons. NS = "non-significant".

Supplementary Figure 3. Establishment of a pilocarpine-induced TLE mouse model

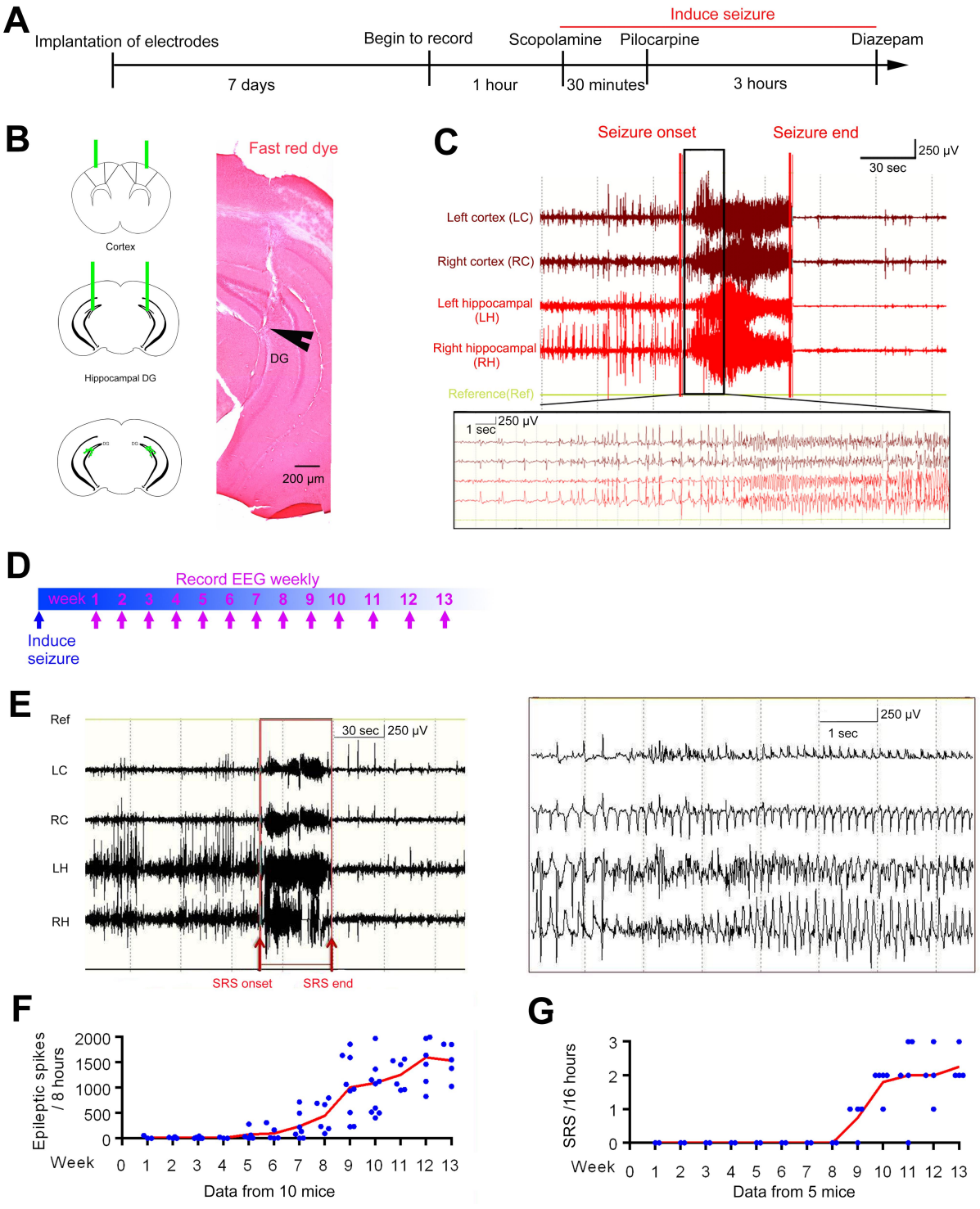

A. Schematic illustration of the experimental paradigm. To induce epilepsy, scopolamine was injected into 2-month-old mice. Fifteen minutes later, pilocarpine was administered to

induce an initial seizure referred to as status epilepticus (SE). SE lasted for 3 hours until seizures were terminated by the injection of diazepam. **B-C.** Induction of SE was monitored by a video/EEG via four electrodes implanted into the hippocampus and motor cortex of the mice. **D-G.** The development of spontaneous epilepsy was continuously monitored by video/EEG. After an approximately 4-week latent period, epileptic spikes were detected 5 weeks post-SE induction (F) and gradually increased over time (n = 10). The occurrence of spontaneous recurrent seizures (SRS) was evident 9 weeks after SE induction (G), and the incidence of SRS also increased over time (n = 5).

Supplementary Figure 4. Repeated CNO treatment alters epileptic phenotypes in an inducible and reversible manner

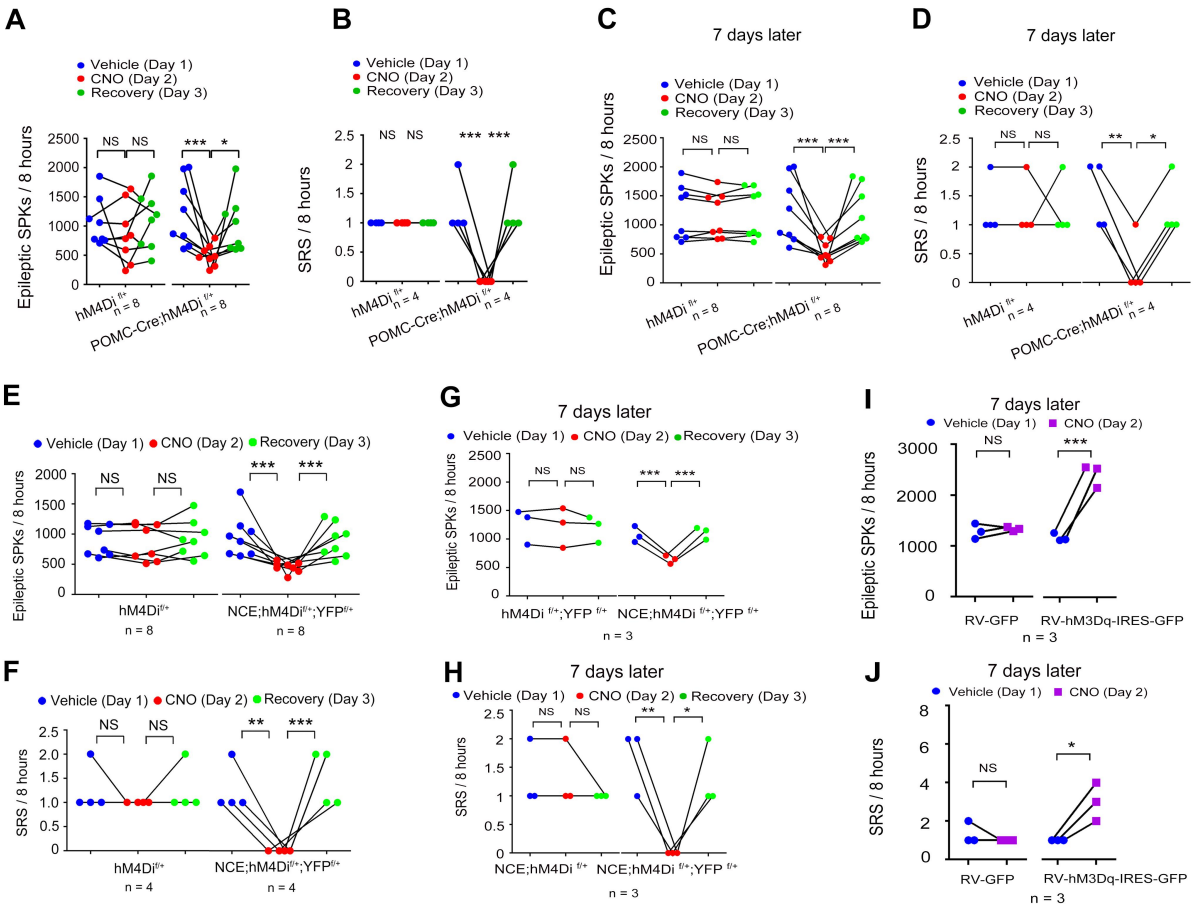

To test the inducibility and reversibility of the DREDD method, we repeated a three-day monitoring process, consisting of day 1 with vehicle treatment, day 2 with CNO injection, and day 3 with an untreated recovery phase, in a 7-day interval. **A-D.** Only CNO treatment significantly reduced both epileptic spikes and SRS in POMC-Cre;hM4Di$^{f/+}$ mice, but not in hM4Di$^{f/+}$ control mice. Mice displayed basal levels of epileptic spikes and SRS during vehicle treatment and recovery. **E-H**. Both epileptic spikes and SRS were significantly reduced in NCE;hM4Di$^{f/+}$;YFP$^{f/+}$ only when treated with CNO. Mice displayed basal levels of epileptic spikes and SRS during vehicle treatment and recovery. **I-J**. On day 1, basal levels of

epileptic spikes and SRS were measured after vehicle treatment. On day 2, CNO significantly increased both epileptic spikes and SRS only in RV-hM3Dq-IRES-GFP-injected mice, but not in RV-GFP-injected control mice. *P<0.05, **P<0.01, and ***P < 0.001, as determined by two-way ANOVAs with Bonferroni's multiple comparisons (A-H) and Wilcoxon matched-pairs signed rank tests (I-J). NS = "non-significant"

Supplementary Figure 5. Hippocampal DGCs are necessary for spontaneous recurrent seizures

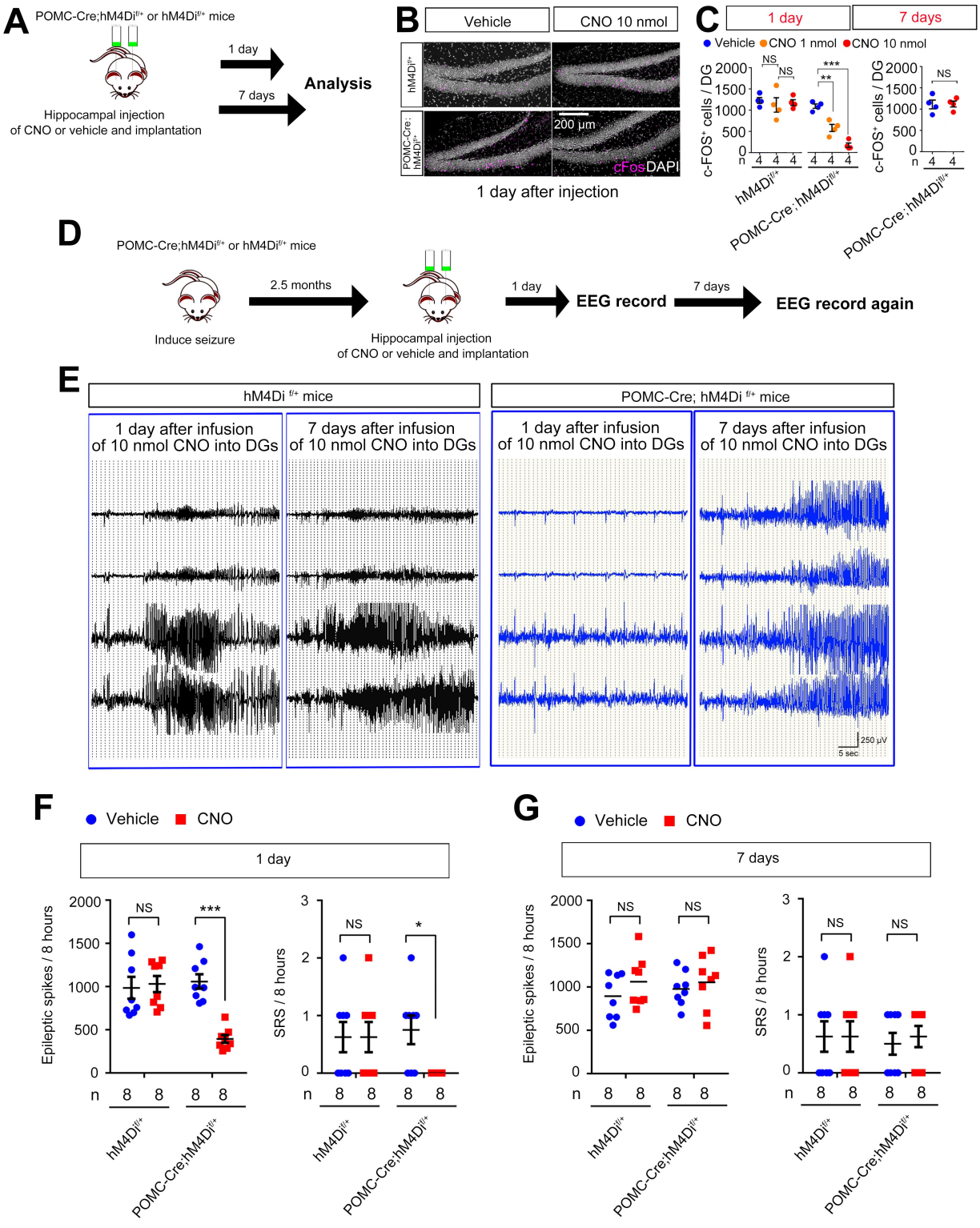

A. Experimental schematic for the direct infusion of CNO into POMC-Cre;hM4Di$^{f/+}$ or hM4Di$^{f/+}$ (control) mice and subsequent analysis 1 day and 7 days later. **B-C.** A direct CNO

infusion into the hippocampus significantly reduced the number of c-FOS^{+} cells in POMC-Cre; hM4Di$^{f/+}$ mice when analyzed 1 day after CNO infusion (B-C), but not 7 days after infusion (C; n = 4, each). **D.** Schematic diagram showing the experimental paradigm to specifically manipulate DGCs in epileptic mice. **E.** Representative EEG recordings show that direct infusion of CNO dramatically reduced SRS 1 day after CNO injection; however, 7 days after CNO, SRS returned to basal levels. **F.** Quantitative results show that direct infusion of CNO into the dentate gyrus significantly reduced the frequency of epileptic spikes and completely blocked SRS in POMC-Cre;hM4Di$^{f/+}$, but not in hM4Di$^{f/+}$, mice. **G.** Epileptic spikes and SRS both returned to basal levels 7 days after CNO administration. Data represent mean ± SEM. *$P < 0.05$, **$P < 0.01$, ***$P < 0.001$, as determined by Kruskal-Wallis non-parametric tests with Dunn's multiple comparison tests (C) and two-way ANOVAs with Bonferroni's multiple comparisons (C, F, and G). NS = "non-significant"

Supplementary Figure 6. Connectivity ratios of newborn DGCs to hilar neurons in epileptic mice

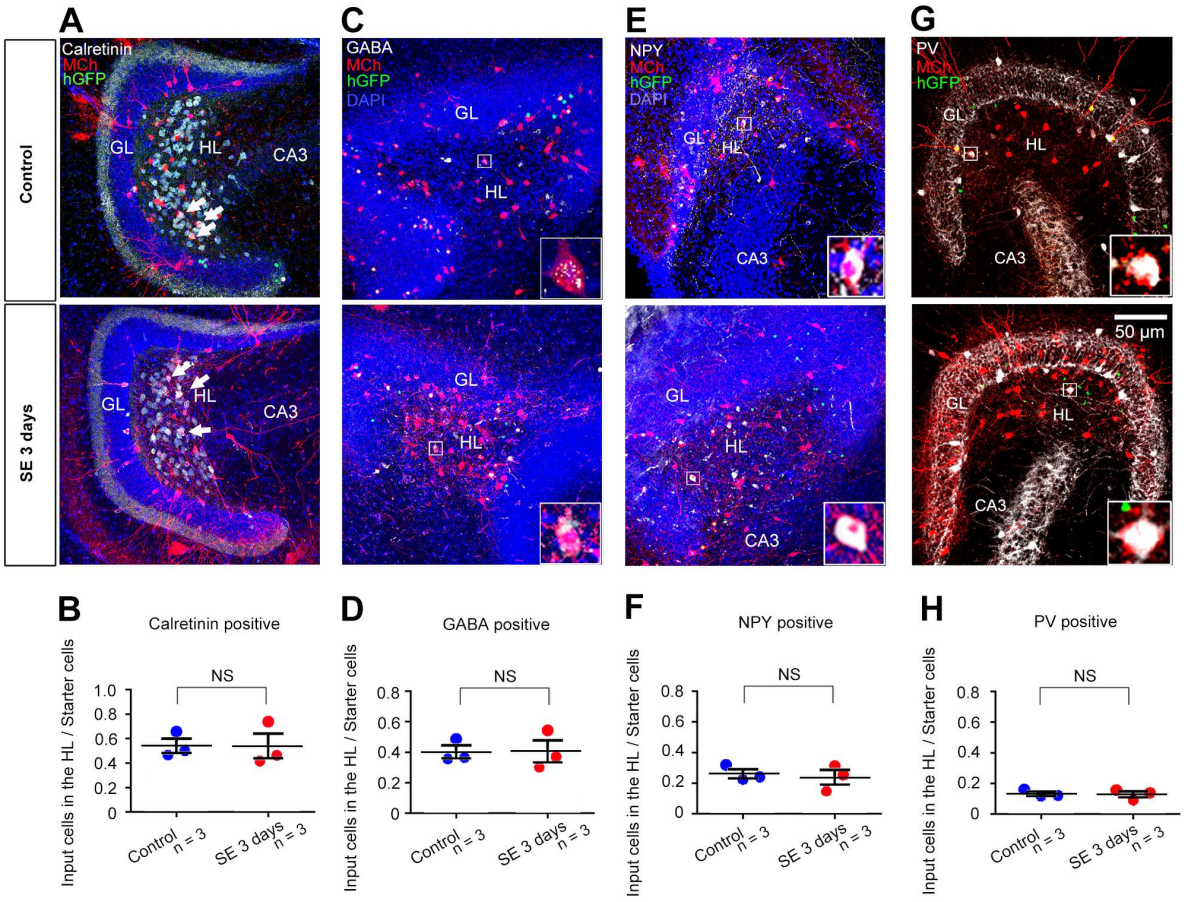

A-B. The connectivity ratios of newborn DGCs to hilar excitatory neurons (Calretinin$^+$ mossy cells) did not change. **C-H**. The connectivity ratios of newborn DGCs to hilar inhibitory neurons positive for GABA, NPY, and PV were not significantly altered in epileptic mice. n = 3 for each group. Data are mean ± SEM. Statistical significance was determined by Mann-Whitney tests (B, D, F, and H). NS = "non-significant"

Supplementary Figure 7. CNO-mediated inhibition of newborn DGCs reduces c-FOS⁺ cells in epileptic mice

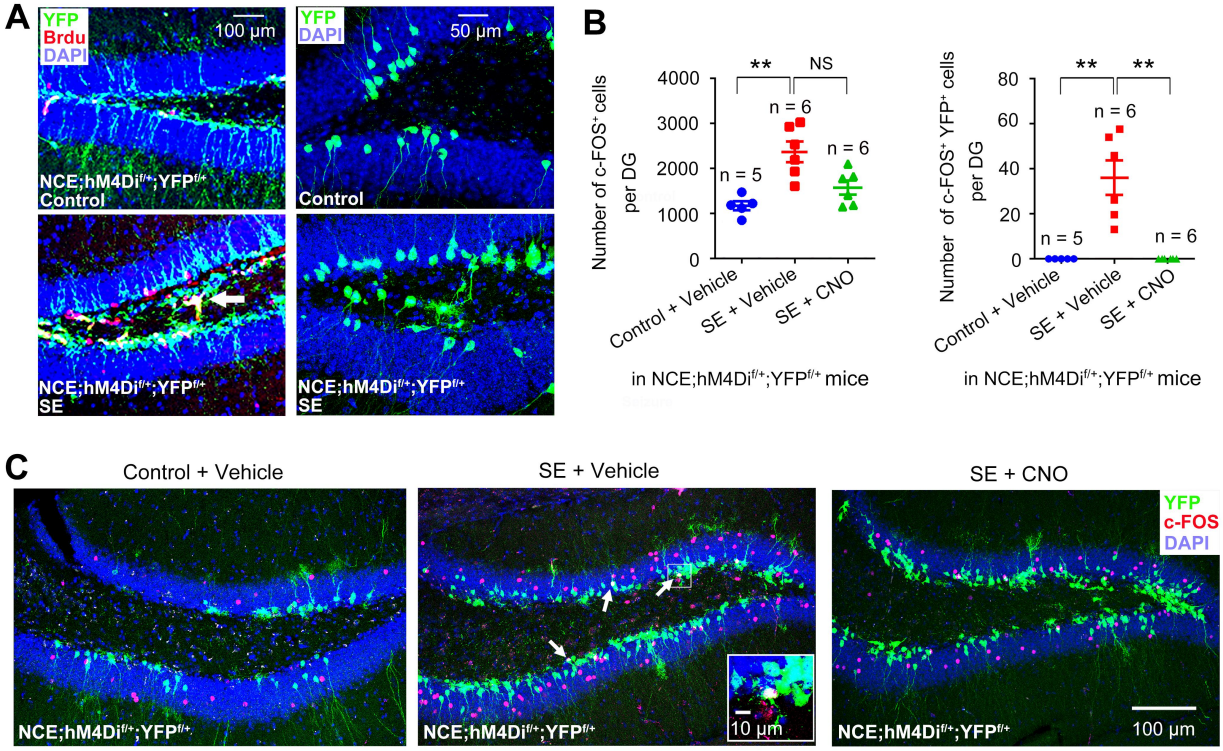

A. Abnormal development and ectopic migration of hippocampal newborn DGCs are shown at 2.5 months after pilocarpine-mediated SE induction. Note the ectopic location of BrdU⁺ (injected 3 days after SE) cells and YFP⁺ cells in the hilus. **B-C.** Specific inhibition of newborn DGCs leads to a reduction in c-FOS⁺ cells in the dentate gyrus of epileptic NCE;hM4Di$^{f/+}$;YFP$^{f/+}$ mice (n = 6, each; n = 5, control). Data are mean ± SEM. $^{**}P < 0.01$ as determined by Kruskal-Wallis non-parametric tests with Dunn's multiple comparison tests (B). NS = "non-significant"

Supplementary Figure 8. hM4Di receptor expression in the brain

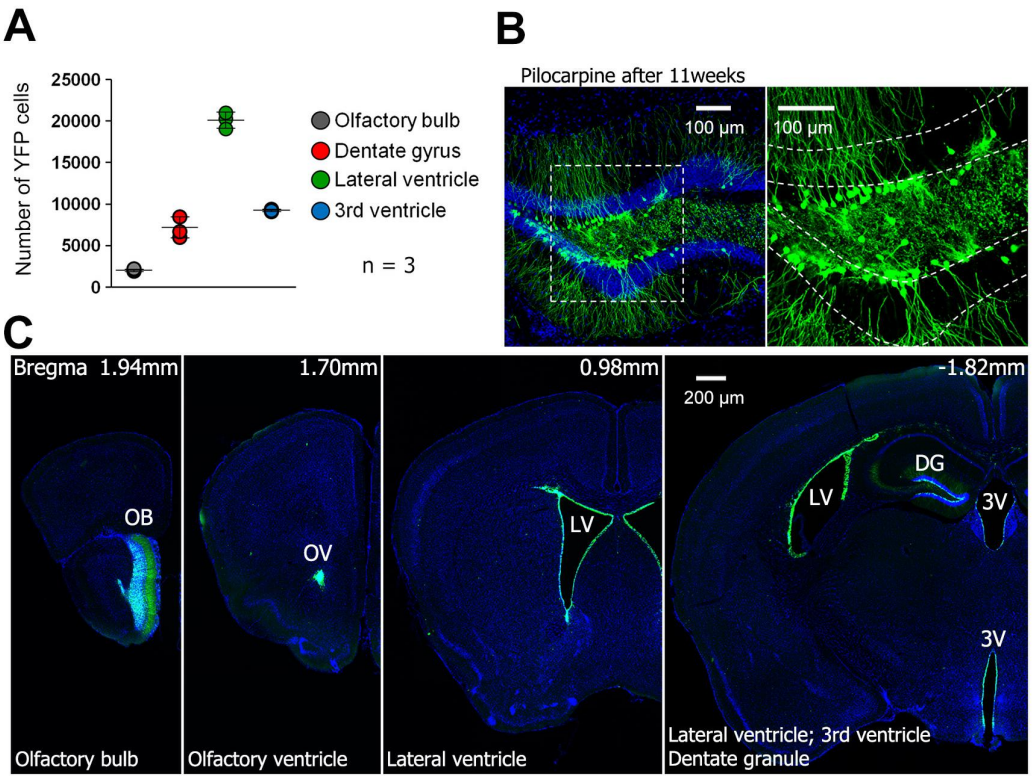

A–C. In addition to the dentate gyrus of the hippocampus, hM4Di receptors are expressed in the subventricular zone, olfactory bulb, and the third ventricle; n = 3. YFP^+ cells were identified mainly in the dentate gyrus of the hippocampus (1200 ± 123), the lateral ventricles (3346 ± 94), the third ventricle (1538 ± 14), and the olfactory bulb (334 ± 14). Data are mean ± SEM.

Supplementary Figure 9. Whole-cell recording shows increased and decreased firing frequencies of newborn DGCs expressing hM3Dq and hM4Di receptors, respectively

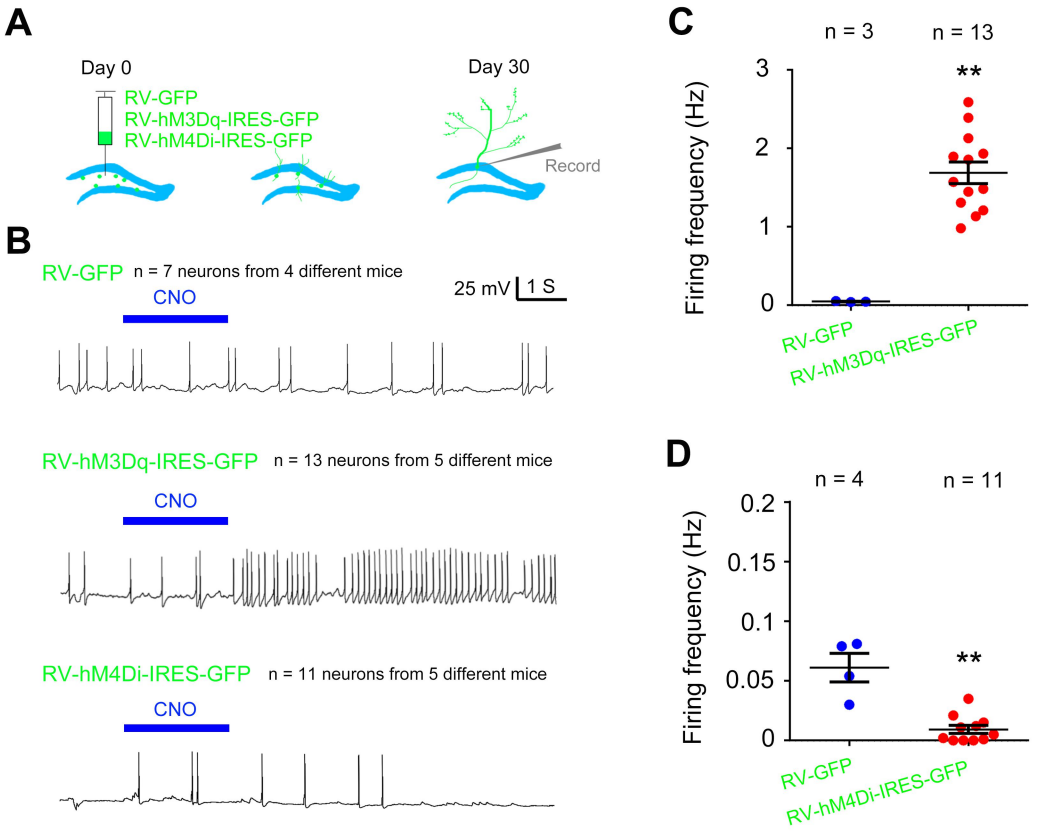

A. Schematic of the experimental paradigm. Retrovirus expressing hM3Dq, hM4Di, or GFP was injected into the dentate gyrus, and whole-cell current clamp recording was performed 30 days later. **B-D.** CNO treatment (10 μM; blue horizontal bar) significantly increased and decreased the firing rate in newborn DGCs expressing hM3Dq and hM4Di receptors, respectively, while the same treatment did not affect the firing rate of GFP-expressing control DGCs. Data represent mean ± SEM. $^{**}P < 0.01$ as determined by Mann-Whitney non-parametric tests.

Supplementary Figure 10. Age-dependent contribution of hippocampal DGCs to epileptic neural circuits

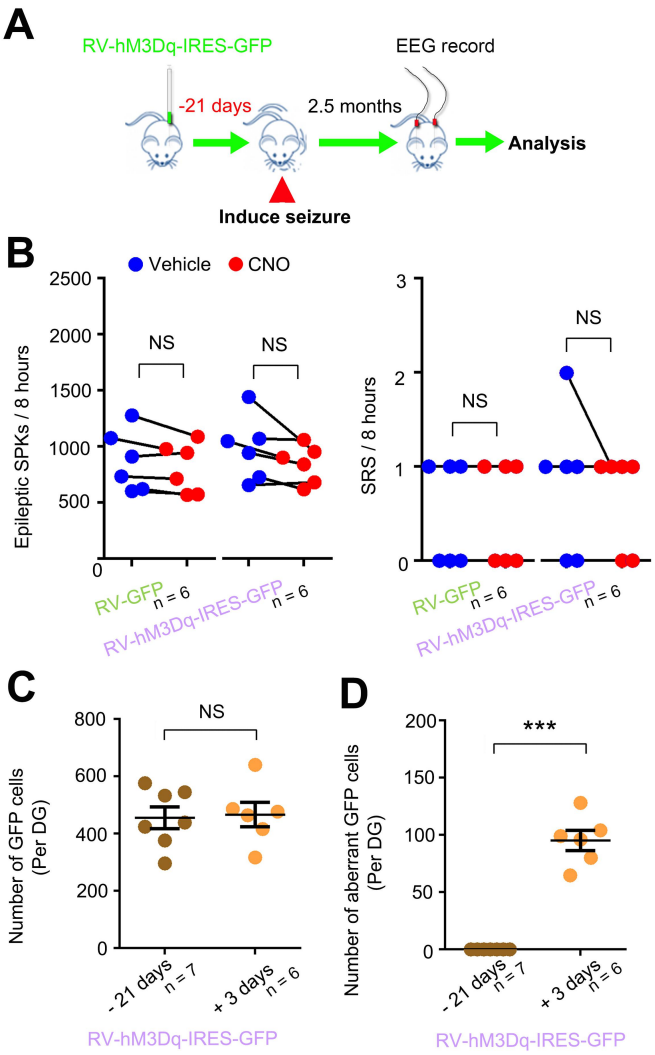

A. A schematic showing the experimental paradigm to determine the role of DGCs born 21 days prior to pilocarpine-mediated SE induction. **B.** In epileptic mice, specific activation of DGCs born 21 days before SE did not significantly affect epilepsy phenotypes such as epileptic spikes and SRS. **C.** The number of hM3Dq receptor-expressing cells as determined by GFP^+ cells was comparable to that of hM3Dq-expressing DGCs that were born 3 days post-SE. **D**. hM3Dq-expressing DGCs born 21 days prior to SE did not show structural

abnormalities. These results suggest that the relative age of DGCs with respect to SE is a critical factor that determines the vulnerability of DGCs to be recruited into pro-epileptic neural circuits. Data represent mean ± SEM. ***$P < 0.001$ as determined by two-way repeated measures ANOVAs with Bonferroni's multiple comparison tests (B) and Mann-Whitney non-parametric tests (C, D). NS = "non-significant"

Experiment	Group	Initial animal number	Lethality	Absence of epileptic spikes	Expression of epileptic spikes	Development of SRS
		All	Excluded	Excluded	Included	Included
Figure 1 B-C	$PDi^{f/+}$	16	5	3	8	4
	POMC-Cre;$PDi^{f/+}$	15	3	4	8	4
Figure 1 D-E	$PDi^{f/+}$	33	10	6	17	9
	POMC-Cre;$PDi^{f/+}$	35	8	8	19	11
Figure 4 D-E	$hM4Di^{f/+}$	31	6	9	16	8
	NCE;$hM4Di^{f/+}$	33	9	7	17	9
Figure 4 F-G	$hM4Di^{f/+}$	16	6	2	8	4
	NCE;$hM4Di^{f/+}$;$YFP^{f/+}$	14	4	2	8	4
Figure 5 G-H	RV-GFP	11	3	1	7	4
	RV-hM4Di-IRES-GFP	14	4	2	8	5
Figure 6 B-C	RV-GFP	10	3	2	5	3
	RV-hM3Dq-IRES-GFP	10	3	1	6	4
Total	Total	238	64	47	127	69

Supplementary Table 1) Summary of included and excluded mice for video/EEG experiments